Two decades of molecular surveillance in Senegal reveal changes in known drug resistance mutations associated with historical drug use and seasonal malaria chemoprevention

Yaye Die NDIAYE[1†] & Wesley WONG[2†], Julie THWING[3], Stephen S SCHAFFNER[4], Abdoulaye TINE[1], Mamadou Alpha DIALLO[1], Awa DEME[1], Mouhammad SY[1], Amy K Bei[5], Alphonse B THIAW[6], Rachel DANIELS[7], Tolla NDIAYE[1], Amy GAYE[1], Ibrahima Mbaye NDIAYE[1], Mariama TOURE[1], Nogaye GADIAGA[1], Aita SENE[1], Djiby SOW[1], Mamane N. GARBA[1], Mamadou Samba YADE[1], Baba DIEYE[1], Khadim DIONGUE[1], Daba ZOUMAROU[1], Aliou NDIAYE[1], Jules GOMIS[1,] Fatou Ba FALL[5], Medoune NDIOP[8], Ibrahima DIALLO[8], Doudou SENE[8], Bronwyn MACINNIS[4], Mame Cheikh SECK[1], Mouhamadou NDIAYE[1], Aida S. BADIANE[1], Daniel L. HARTL[9], Sarah K. VOLKMAN[2,4,10], Dyann F. WIRTH[2,4,*], Daouda NDIAYE[1,2,*]

†: these authors contributed equally

*corresponding authors

Affiliations

1. International Research Training Center on Genomics and Health Surveillance (CIGASS), Cheikh Anta Diop University, Dakar, 16477, Senegal

2. Department of Immunology and Infectious Diseases, Harvard T.H. Chan School of Public Health, 665 Huntington Ave, Boston, MA, 02115, USA

3. Centers for Disease Control and Prevention, 1600 Clifton Road, Atlanta, GA ,30329, USA

4. Broad Institute of MIT and Harvard, 415 Main Street, Cambridge, MA, 02142, USA

5. Yale School of Public Health, 60 College St, New Haven, CT 06510

6. Department of biochemistry and Functional Genomics, Sherbrooke University, 2500 Bd de l'Université, Sherbrooke, QC J1K 2R1, Canada

7. RNA Therapeutics Institute, UMass Chan Medical School, 368 Plantation Street, Worcester MA 01605

8. National Malaria Control Program (NMCP), Rue FN 20, Dakar 25270, Senegal

9. Department of Organismic and Evolutionary Biology, Harvard University, 16 Divinity Avenue, Cambridge, MA, 02138 USA

10. Simmons University, 300 The Fenway, Boston, MA, 02115, USA

34

35 **ABSTRACT**

36 Drug resistance in *Plasmodium falciparum* is a major threat to malaria control efforts. We

37 analyzed data from two decades (2000-2020) of continuous molecular surveillance of *P.*

38 *falciparum* parasite strains in Senegal to determine how historical changes in drug

39 administration policy may have affected parasite evolution. We profiled several known drug

40 resistance markers and their surrounding haplotypes using a combination of single

41 nucleotide polymorphism (SNP) molecular surveillance and whole-genome sequence (WGS)

42 based population genomics. We observed rapid changes in drug resistance markers

43 associated with the withdrawal of chloroquine and introduction of sulfadoxine-pyrimethamine

44 in 2003. We also observed a rapid increase in *Pfcrt* K76T and decline in *Pfdhps* A437G

45 starting in 2014, which we hypothesize may reflect changes in resistance or fitness caused

46 by seasonal malaria chemoprevention (SMC). Parasite populations evolve rapidly in

47 response to drug use, and SMC preventive efficacy should be closely monitored.

48

49 **INTRODUCTION**

50 The World Health Organization (WHO) estimated 247 million malaria cases and

51 619,000 deaths in 2021[1]. Children under 5 years of age are the most vulnerable to malaria,

52 accounting for 80% of deaths worldwide; 96% of malaria cases and deaths in 2021 were in

53 the African region[1]. Increased funding for malaria control has led to an estimated 30%

54 reduction of malaria mortality since 2000, using a combination of vector control and drug-

55 based interventions[2]. However, the development of parasite resistance to antimalarials

56 threatens to undermine control and elimination efforts and poses a significant threat to public

57 health.

58 Therapeutic efficacy studies (TES) are the gold standard for evaluating clinical and

59 therapeutic drug efficacy[3,4]. TES are prospective evaluations of patients' clinical and

60 parasitological responses to treatment as assessed 28 or 42 days after treatment. However,

61   TES are resource intensive and can be challenging to implement where transmission is low[5].

62   Furthermore, antimalarial drugs may also be used as chemoprophylaxis to prevent infection.

63   WHO-recommended chemopreventive strategies include intermittent preventive treatment for

64   pregnant women (IPTp) and infants (IPTi), seasonal malaria chemoprevention (SMC), and

65   mass drug administration (MDA)[1,6]. As with TES, chemopreventive efficacy studies can be

66   challenging to implement and require significant planning and longitudinal monitoring[7].

67   Parasite drug resistance is a major factor that influences therapeutic and

68   chemopreventive antimalarial efficacy. Molecular surveillance of genetic markers could be

69   used to detect emerging drug resistance or changes in parasite fitness [8–13] that could

70   undermine therapeutic or chemopreventive efficacy. Molecular surveys of drug resistance

71   commonly focus on assessing the frequency of single nucleotide polymorphisms (SNPs) or

72   copy number variations that have been associated with drug resistance in laboratory

73   settings[1,13]. Scanning the genomic regions and haplotypes surrounding these mutations for

74   evidence of hard or soft selective sweeps also provides insight into the origins of these

75   mutations and provides additional evidence of drug selection at these sites[13,14]. Selective

76   sweeps occur when mutations become fixed or are eliminated so rapidly that it causes a

77   reduction in the variation at nearby nucleotide positions[13,14]. Hard selective sweeps indicate

78   selection from a single genomic background, while soft selective sweeps indicate selection

79   from multiple backgrounds or pre-existing standing variation.

80   In this study, we examined a two-decade collection of *P. falciparum* samples

81   collected from febrile individuals in Senegal to assess how historical changes in drug use has

82   affected the parasite population. Based on the historical antimalarial policy in Senegal, we

83   focused our analyses on SNPs associated with resistance to chloroquine (CQ), amodiaquine

84   (AQ), sulfadoxine-pyrimethamine (SP), and artemisinin (ART). We were also interested in

85   using molecular surveillance to look for signs of emerging drug resistance or changes in

86   parasite fitness that could signal a reduction in IPTp or SMC chemopreventive efficacy in

87   Senegal. In Senegal, IPTp is administered as a dose of SP to pregnant women during

88   antenatal care visits and is spaced at least 30 days apart. A single cycle of SMC consists of

89   a dose of SP + AQ on the first day, followed by doses of AQ on days 2 and 3. In Senegal,

90   children 3 months to 10 years are targeted, with three to five monthly cycles during the

91   transmission season, depending on the length of the transmission season in their region.

92

93   **RESULTS**

94   **Study design and SNP-based molecular surveillance sampling**

95   *P. falciparum* samples from febrile patients collected between 2000-2020 were

96   genotyped. A total of 3,284 samples were collected from six regions of Senegal: Pikine,

97   Thiès, Kedougou, Diourbel, Kaolack, and Kolda (**Figure 1A**). Kedougou and Kolda are high

98   transmission regions in southeast Senegal. In 2021, reported annual incidence was 536.5

99   cases per 1000 in Kedougou and 214.5 cases per 1000 in Kolda[15]. SMC has been

100   implemented in Kedougou and Kolda since 2014. Kaolack (10.9 cases per 1000) and

101   Diourbel (19.4 cases per 1000) are intermediate transmission regions in central Senegal, and

102   started SMC in 2019. Thiès (2.8 cases per 1000) and Pikine (4.9 cases per 1000) are low

103   transmission sites in western Senegal. SMC is not implemented in Thiès or Pikine.

104   Our sample collection spans several important changes in official drug use policy (**Fig

105   1B**). These changes include the withdrawal of CQ and the introductions of SP, AQ, and

106   artemisinin-based combination therapies (ACTs). Based on this drug policy history, we

107   examined several SNP-based drug resistance markers in *Pfcrt*, *Pfdhfr*, *Pfdhps*, *Pfmdr1*, and

108   *Pfklech13* (**Table 1**). Because resistance to pyrimethamine involves multiple mutations in

109   *Pfdhfr*, we examined the frequency of *Pfdhfr* triple mutant CRN (mutant at N51C, C59R, and

110   S108N)[16] and "quadruple" mutants (*Pfdhfr* triple mutant CRN + *Pfdhps* A437G). Likewise, we

111   examined the frequency of the *Pfmdr1* NFD (N86Y, Y184F, D1246Y) haplotype because the

112   haplotype is associated with resistance against multiple drugs[17,18].

113   Our sample collection varied throughout time and space (**Fig S1**). The 444 samples

114   collected between 2000 and 2005 came exclusively from Pikine, the 800 samples collected

115   between 2006 and 2014 came from Thiès, and the 340 samples collected between 2015 and

116   2017 came from Kedougou. Between 2017 and 2020, 1700 samples were collected from

117   Thiès, Kaolack (starting in 2020), Diourbel, Kolda (starting in 2019), and Kedougou.

118   **Molecular surveillance detects rapid changes in *Pfcrt, Pfdhfr, Pfdhps*, and**

119   ***Pfmdr1* mutations over time**

120   The changes in sampling numbers and locations over time presented a unique

121   challenge. We first examined the population frequencies of each SNP in the sample regions

122   with more than three years of continuous sampling: Pikine, Thiès, and Kedougou (**Fig S2-**

123   **S4**). Pikine and Thies are urban sites with low transmission that have not implemented SMC

124   while Kedougou is a rural site with high transmission that has been implementing SMC since

125   2014.

126   We noted that the data from Pikine and Thiès (which are approximately 30 miles

127   apart) prior to 2014 appeared to be part of a continuous time series and that changes in

128   Thiès and Kedougou after 2014 followed similar trends. To summarize the molecular

129   surveillance data and identify broad changes in mutation frequency, we used a binomial

130   generalized additive model (GAM) to identify and highlight Senegal-wide trends in mutation

131   frequency (**Methods**, **Fig 2**).

132   *Increase in Pfcrt* K76T *mutation frequency after 2014*

133   As expected, due to a fitness cost associated with *Pfcrt K76T,* we observed a decline

134   in *Pfcrt K76T* mutation frequency between 2000 and 2014 following the withdrawal of CQ in

135   2003. Unexpectedly, this was followed by an increase in frequency after 2014. In 2000, our

136   model estimated a Senegal-wide mutation frequency of 0.76 (95% CI 0.59 - 0.87), which fell

137   to 0.26 (95% CI0.21 - 0.31) in 2014. However, the frequency began rising after 2014, and the

138   model estimated the frequency to be 0.49 (95% CI 0.41 - 0.57) in 2020. The adjusted *R*-

139   squared for the model was 0.466 and the deviance explained 54.2%.

140   When examined separately, there was a statistically significant increase in *Pfcrt* K76T

141   in both Thiès (p-value < 0.00001) and Kedougou (p-value = 9.6e-5) after 2014. When

142   examining the sites not included in the Senegal-wide GAM (Kolda, and Kaolack), the

143   frequency of *Pfcrt K76T* were consistent with those predicted by the GAM. However, the

144   frequency of *Pfcrt K76T* in Diourbel trended in the opposite direction, declining from 0.45

145   (95% CI 0.55 - 0.40) to 0.20 (95% CI 0.11 - 0.29) and 0.22 (95% CI 0.13 - 0.31) in 2018,

146   2019, and 2020, respectively.

147   *Changes in Pfdhfr triple mutants following the withdrawal of CQ and introduction of SP*

148   We expected an increase in *Pfdhfr CRN* triple mutants due to pyrimethamine

149   exposure from either SP therapy beginning in 2003 or IPTp chemoprevention beginning in

150   2004. Our data show a sharp rise in the frequency of *Pfdhfr* triple mutants starting in 2003,

151   coinciding with the replacement of CQ with SP as the first-line antimalarial treatment in

152   Senegal (**Fig 2B**). The increase in the *Pfdhfr* triple mutant corresponded to a decrease in

153   *Pfdhfr* triple sensitives (*N51N, C59C, S108S*) (**Fig S5A**) and we detected only a few

154   parasites with a mix of *Pfdhfr N51N, C59C, S108S* status. In 2003, the GAM predicted that

155   the frequency of triple mutants in Senegal was 0.42 (95% CI 0.27 - 0.59). By 2020, the

156   predicted frequency was 0.95 (95% CI 0.90 - 0.97). The adjusted R-squared and deviance

157   explained by the model were 0.881 and 89.4%.

158   *Rise and fall of Pfdhps* A437G *before and after SMC expansion in 2014*

159   We expected mutations in *Pfdhps* to increase due to sulfadoxine exposure from either

160   SP therapy or IPTp chemoprevention or SMC. *Pfdhps* K540E, A581G, A613T/S were rare (<

161   5%) or undetected by our sampling and only *Pfdhps* A437G was detected at high

162   frequencies (**Fig 2C, Fig S2-S4**). Unlike with the *Pfdhfr* triple mutants, the *Pfdhps A437G*

163   allele trajectory and "quadruple" mutant haplotype trajectory changed directions multiple

164   times (**Fig S5B**). Our data revealed several inflection points (at 2003, 2008, and 2014) where

165   the trajectory of *Pfdhps* prevalence changed.

166   Between 2000 and 2003, we observed an increase in *Pfdhps* A437G from the GAM-

167   predicted frequency of 0.26 (95% CI 0.14 - 0.44) in 2000 to 0.47 (95% CI 0.19 - 0.77) in

168   2003. After 2003, *Pfdhps* A437G decreased until 2008, when its predicted frequency was

169   0.17 (95% CI 0.11 - 0.27). Between 2008 and 2014, the frequency of *Pfdhps A437G* rose

170   until 2014, when its predicted mutation frequency was 0.72 (95% CI 0.58 - 0.83). After 2014,

171   the frequency of *Pfdhps* A437G declined, and the predicted mutation frequency in 2020 was

172   0.33 (95% CI 0.25 - 0.40). Overall, the adjusted *R*-squared and deviance explained by the

173   model were 0.554 and 69.1%, respectively.

174   *Molecular surveillance detects changes in Pfmdr1* NFD *haplotype over time*

175   Expectations for the *Pfmdr1* NFD were less certain as mutations in *Pfdmr1* have been

176   associated with resistance against multiple drugs. Between 2008 and 2012, we observed a

177   rapid increase in the *Pfmdr1* NFD (N86Y, Y184F, D1246Y) haplotype (**Fig 2D**). The

178   corresponding model-predicted frequencies were 0.27 (95% CI 0.20 - 0.37) in 2004 and 0.74

179   (95% CI 0.57 - 0.79) in 2012. After 2012, the predicted frequency of the *Pfmdr1* NFD

180   haplotype declined to 0.56 (95% CI 0.48 - 0.63) in 2016, where it remained relatively stable

181   until 2020 [0.56 (95% CI 0.49 - 0.63)]. The adjusted *R*-squared and deviance explained by

182   the model were 0.817 and 87.2%, respectively.

183   *Infrequent detection of Pfkelch13 A578S and absence of Pfkelch13 C580Y in Senegal*

184   *Pfkelch13* C580Y was not detected in our samples, while *Pfkelch13 A578S* was

185   present but infrequently detected (**Fig 2E-F**). The *Pfkelch13* A578S mutation was observed

186   in one of the 89 genotyped samples collected from Kedougou in 2015 and twice in the 123

187   genotyped samples collected from Kedougou in 2017, but in no other year. The *Pfkelch13*

188   C580Y mutation was not detected in any of our genotyped samples.

189　*Genomic haplotype analyses reveal differences in selection acting on Pfcrt, Pfdhps,* and

190　*Pfdhfr*

191　　　　To determine whether the changes in *Pfcrt*, *Pfdhps*, and *Pfdhfr* resulted from drug-

192　mediated selection, we examined the genomic haplotypes surrounding these genes in a set

193　of 231 whole genome sequences collected from Thiès and Kedougou between 2006 and

194　2019 (**Fig S6**). Our primary goal was to determine whether *Pfcrt* K76T, *Pfdhps* A437G, and

195　the *Pfdhfr* triple mutant CRN showed evidence of a rapid selective sweep indicative of strong

196　drug pressure by examining the haplotype diversity in the surrounding genomic regions.

197　*Pfmdr1* was not examined because of its strong potential for copy number variation.

198　　　　For *Pfcrt* K76T, we found strong evidence of a selective sweep. The haplotype

199　structure surrounding *Pfcrt* K76T was far less diverse than that surrounding the ancestral

200　*Pfcrt* K76 (**Fig 3A-B**). *Pfcrt* K76 haplotypes rapidly diversified within the first 20kb. In

201　contrast, *Pfcrt* K76T was surrounded by a dominant extended haplotype to its left (upstream)

202　and two major extended haplotypes to its right (downstream). These dominant haplotypes

203　extended out nearly 50 kb away from the *Pfcrt* K76T locus and included parasites collected

204　before and after 2014. The extended haplotype homozygosity (EHH) for *Pfcrt* K76T was

205　elevated relative to *Pfcrt* K76 (**Fig 3C**).

206　　　　For *Pfdhps*, we surprisingly found little evidence of a hard selective sweep (selection

207　of a single or small number of haplotypes). Instead, the haplotype structure surrounding the

208　sensitive and resistant alleles were highly diverse and there was no significant elevation in

209　EHH (**Fig 3D-F**). Multiple long-range haplotypes extended outwards from either *Pfdhps*

210　A437G or *Pfdhps* A437A for 30-50 kb. Combined with the changes in allele frequency

211　observed in the molecular surveillance, we wanted to determine whether *Pfdhps* A437G

212　showed evidence of being selected for but across multiple competing backgrounds (a "soft"

213　sweep)[19]. To test this, we adapted two existing statistical measures of selection, H12 and

214　H2/H1. H12 is the expected haplotype homozygosity, treating the two most common

215　haplotypes as if it were a single haplotype, and H2/H1, the ratio of the second and the first

216   most frequent haplotype (**Fig S7**)[20]. Elevated H12 and a low H2/H1 ratio indicates a hard

217   selective sweep while elevated H12 and a high H2/H1 ratio suggests a soft selective sweep

218   (**Methods**). We found that, compared to the rest of chromosome 8, both H12 and the H2/H1

219   ratio around *Pfdhps* were elevated (**Fig S7A**), consistent with a soft sweep. Conversely, H12

220   around *Pfcrt* was high but H2/H1 was low, indicating a harder selective sweep (**Fig S7B**).

221   We detected a strong extended haplotype structure surrounding the *Pfdhfr* triple

222   mutant. Most *Pfdhfr* triple mutants shared the same dominant haplotype (**Figure 3 G-I**). This

223   haplotype extended out more than 50 kb to the left of the *Pfdhfr* gene and 20 kb to the right.

224   The EHH of the *Pfdhfr* was likely due to a hard selective sweep, similar to that detected for

225   *Pfcrt* K76T. However, we lacked the sensitivity to accurately estimate the EHH surrounding

226   the *Pfdhfr* triple sensitive genotype. Most samples with usable *Pfdhfr* sequences were

227   collected after 2010 (**Fig S5C**), after the rapid increase in the *Pfdhfr* triple mutant identified

228   by our SNP-based molecular surveillance (**Fig 2C**). *Pfdhfr* triple mutants comprised 0.83

229   (95% CI 0.77 - 0.89) of our whole genome sequenced samples; 0.07 (95% CI 0.03 - 0.11)

230   were mixed mutants, and only 0.10 (95% CI 0.05 - 0.14) of our samples were *Pfdhfr* triple

231   sensitive parasites.

232   *Haplotype analyses reveal temporal changes in selection at Pfcrt* K76T *before and after 2014*

233   For *Pfcrt* K76T, we also estimated the EHH before and after SMC to determine

234   whether SMC could be driving the selective sweep (**Fig 4**). Prior to 2014, the EHH directly

235   proximal to the *Pfcrt* K76T resistance mutation was similar to that observed surrounding the

236   sensitive *Pfcrt* K76. However, we detected elevated EHH 10 kb upstream and downstream of

237   the *Pfcrt* K76T locus, which is likely a legacy of the historical selective sweep that occurred

238   prior to CQ withdrawal in 2003 (**Fig 4B**)[21]. After the introduction of SMC in 2014, the EHH

239   surrounding *Pfcrt* K76T was elevated (**Fig 4A, C**) and consistent with the expectations for a

240   new selective pressure acting on the mutation occurring after 2014.

241   **DISCUSSION**

242   Accurate assessments of drug resistance in parasite populations are needed to

243   ensure continued success of drug-based malaria control efforts. The changes in the

244   frequency of *Pfdhfr* triple mutant CRN suggest that pyrimethamine resistance is widespread

245   throughout Senegal. Nearly all parasites carried the *Pfdhfr* triple mutant by 2013. The

246   increase in *Pfdhfr* triple mutant is consistent with pyrimethamine-mediated drug resistance,

247   first from antimalarial SP therapy, and then from chemopreventive IPTp. A similar rise in

248   *Pfdhfr* triple mutant frequency was previously reported by a study carried out in Thiès in 2003

249   and 2013[22,23]. Our haplotype analysis suggests that SP-mediated pyrimethamine increase in

250   *Pfdhfr* triple mutant occurred rapidly from a single haplotype.

251   Changes in *Pfcrt K76T* and *Pfdhps A437G* were more complex but coincided with

252   several important changes in either therapeutic or chemopreventive drug use. In 2003,

253   Senegal stopped recommending CQ as the first-line antimalarial therapy due to widespread

254   CQ resistance across the African continent[21,24,25]. Although *Pfcrt K76T* is associated with CQ

255   resistance, it confers a fitness cost in *in vitro* laboratory settings where CQ is absent[26]. The

256   decline in *Pfcrt* K76T reported in our study is consistent with other molecular surveillance

257   studies that have shown similar declines in frequency after the withdrawal CQ[27,28] and similar

258   reductions in EHH (**Figure 4B**) surrounding the *Pfcrt* K76T mutation as parasites begin

259   outcrossing more frequently with CQ sensitive parasites[29,30].

260   The increase in *Pfcrt* K76T in 2014 was unexpected but our haplotype analyses

261   suggest that the increase in frequency is due to a new selection event occurring after 2014.

262   These changes coincide with the implementation and expansion of SMC in the high

263   transmission regions of Senegal. We suspect the sudden increase in *Pfcrt* K76T may be

264   being driven by the AQ used in SMC and by the introduction of ASAQ, one of the first line

265   ACTs in use in Senegal. Laboratory based studies have shown that the mutation confers AQ

266   resistance and previous molecular surveillance studies have associated the mutation with

267   AQ resistance [31,32]. In Nigeria, AQ monotherapy may explain the high frequencies of *Pfcrt*

268   K76T despite the withdrawal of CQ[33]. Despite these findings, recent TES studies in Senegal

269   show that ASAQ remained highly efficacious in 2020[34]. The therapeutic efficacy of ASAQ

270   should be closely monitored, as our data suggest that molecular evidence of AQ resistance

271   is increasing in Senegal. Efforts to ensure that ASAQ is not used for treatment in areas in

272   which SMC is in use are critical.

273   Likewise, the rapid frequency changes at *Pfdhps* A437G was unexpected and is a

274   reversal of the accumulation of "quadruple" mutant parasites (parasites that are *Pfdhfr* triple

275   mutant and *Pfdhps* A437G) observed in African countries where SP is administered[35]. These

276   results suggest that Senegal parasites may be more sensitive to sulfadoxine relative to the

277   quadruple mutant parasites observed in other African countries. It is unclear what is driving

278   this decrease in *Pfdhps A437G*, but we hypothesize that it is related to an AQ-induced fitness

279   cost. This hypothesis is based primarily on the decline in *Pfdhps* A437G shortly after the

280   implementation of SMC in 2014 but could also explain the decline in *Pfdhps* A437G

281   frequency between 2003 and 2008 when SP-AQ and ASAQ were used for antimalarial

282   therapy. The increase between 2008 and 2014 could be because antimalarial therapies have

283   increasingly relied on Artemether Lumefantrine (Coartem/AL) after its introduction in 2008[36].

284   Determining whether the changes in *Pfcrt* and *Pfdhps* are the result of the SP and AQ

285   dynamics as administered in SMC will require *in vitro* and *in vivo* phenotypic validation. The

286   hypotheses raised in this study will also need to be recontextualized with comprehensive

287   models of drug resistance that consider how drug resistance mutations change in

288   populations with multiple drug recommendations and regimens[37,38]. This is particularly

289   relevant for interpreting the changes in *Pfmdr1,* where a variety of mutations and copy

290   number variations have been shown to modulate resistance against multiple drugs[2,18]. While

291   the *Pfmdr1* NFD haplotype has been used as a surrogate marker for AQ and lumefantrine

292   resistance[39,40], the observed changes in haplotype frequency likely reflect the combined

293   impact of multiple drugs (**Fig 2D**). Dissecting the factors driving the changes in *Pfmdr1* and

294   their implications for future therapeutic and chemopreventive strategies is a subject for future

295   study.

296   Model-based assessments of mutation frequency would also be helpful for

297   determining why post-2014 changes in *Pfdhps* A437G and *Pfcrt* K76T were observed in both

298   SMC (Kedougou) and non-SMC regions (Thiès). One possibility is that the changes

299   represent two separate selection events occurring in Thiès and Kedougou. The sharp

300   increase in Thiès could be the result of unofficial CQ use or use of CQ for COVID-19

301   prevention or treatment in 2020[41]. However, the rise in *Pfcrt* K76T predates COVID-19, and

302   we are unaware of any factors that might have caused a major shift in unofficial CQ use in

303   2014. Alternatively, this could indicate that the parasite populations in Senegal are

304   interconnected and that parasites from SMC regions are being exported to non-SMC regions.

305   Connectivity between Kedougou and Thiès is supported by the appearance of the major

306   post-2014 *Pfcrt* K76T haplotypes at both sampling sites. Reports from the 2014 Senegal

307   census show significant levels of human movement from the higher transmission,

308   southeastern corner of the country (in which Kedougou is located) to the lower transmission

309   western sections of the country (in which Thiès is located)[42]. Incorporating travel history

310   surveys into molecular surveillance may help determine to what extent parasite populations

311   are interconnected.

312   A major limitation of our study was that sample collection was uneven across space

313   and time. To summarize the data, we combined the data into a single, Senegal-wide model

314   based on the drug resistance marker data from Pikine, Thiès, and Kedougou. This approach

315   assumes each study site represents a sampling from a greater, well-mixed parasite

316   population. When examined separately, the data from each site followed the same temporal

317   trends. In this study, evidence of a single, admixing parasite population included 1) the fact

318   that Pikine and Thiès are geographically proximal (~30 miles), 2) the post-2014 mutation

319   frequencies in Thiès and Kedougou follow similar trajectories, and 3) the mutation

320   frequencies observed in sites not included in the model (Kolda, and Kaolack) tended to be

321   consistent with the model predictions. Previous parasite population genetic analyses in

322   Senegal based on the time-serial allele frequency data of neutral sites and Fst from *msp-*

323   typing have consistently suggested a well-mixed parasite population[43,44]. While we cannot

324   exclude the possibility of site-specific differences in mutation frequency, there is little

325   evidence that the parasite population genetic structure in Senegal is as fragmented as those

326   seen in the Greater Mekong region of Southeast Asia[45].

327   Likewise, our limited surveillance of the *Pfkelch13* limits our conclusions regarding

328   artemisinin resistance in Senegal. Although we did not detect significant levels of either

329   *Pfkelch13* C580Y or *Pfkelch13* A578S in Senegal, we did not examine the other mutations

330   associated with delayed clearance in the *Pfkelch13* propeller domain in our SNP-based

331   molecular surveillance[46–48] or the *Pfkelch13* C439Y and A675Y mutations observed in

332   Uganda[49–51]. Expanding molecular surveillance to include amplicon-based[52] approaches to

333   genotype the entire Pfkelch13 propeller domain would allow for better assessments of

334   growing artemisinin resistance risk in Senegal.

335   To summarize, our molecular surveillance suggests widespread pyrimethamine

336   resistance in Senegal and shows signs of emerging AQ resistance after the introduction of

337   SMC due to an increase in *Pfcrt K76T*. Unusually, we detected a recent decrease in *Pfdhps*

338   A437G, which could indicate a return to sulfadoxine susceptibility, which we hypothesized is

339   due to a yet uncharacterized fitness cost when AQ is present. Given the increased drug

340   pressure associated with using the same drug for both treatment and prevention, we

341   recommend that AQ not be used as a partner drug in artemisinin combination therapies in

342   SMC-treated regions (consistent with WHO recommendations) and that the chemopreventive

343   efficacy of SMC be closely monitored[53].

344   **METHODS**

345   Sampling

346   Parasite samples were collected from treatment seeking patients aged 3 months or older

347   presenting with fever or history of fever within the past 48 hours in Pikine, Thiès, Kedougou,

348   Diourbel, Kolda, and Kaolack between 2000 and 2020. Informed consent was administered

349   (to parents or guardians if the patient was a minor). All patients with positive tests received

350   free malaria treatment with AL or ASAQ, in accordance with the National Health

351   Development Policy in Senegal as recommended by WHO.

352   In addition to slide preparation and RDT, all consenting patients also gave a finger stick

353   blood sample spotted on filter paper (Whatman Protein Saver FTA-about five drops). After

354   drying, samples were stored in plastic bags at room temperature and protected with silica gel

355   desiccant for later DNA isolation for molecular testing.

356   **Laboratory procedures**

357   **Sample collection and DNA extraction**

358   A total of 3,284 DNA samples were extracted from blood spots collected on Whatman

359   Protein Saver FTA-filter papers (Whatman® 3MM CHR CAT N° 3030-662) using QIAamp

360   DNA Mini Kit (QIAGEN, Valencia, CA, USA), according to manufacturer's directions.

361

362   **High Resolution Melting**

363   Drug resistance markers in *Pfcrt*, *Pfmdr1*, *Pfdhfr*, *Pfdhps* were assessed using High

364   Resolution Melting (HRM) assay with the Roche LightCycler 96 instrument (Roche Molecular

365   systems) as previously described[54]. The HRM assay was set up in a total volume of 5 μl

366   containing 2.5 μl of DNA and 2.5x LightScanner mastermix LCGreen (Plus double-stranded

367   DNA dye (Idaho Technology, Inc.)). The codons 76 in *pfcrt* gene; 86, 184, 1042, 1246 in

368   *pfmdr1* gene; 51, 59, 108 in *pfdhfr* gene; 437, 540, 581, 613 in *pfdhps* gene were used. The

369   following reference DNA strains were used: 3D7 (*Pfmdr1 NYD*; *Pfcrt* K76; *Pfdhfr* N51, C59,

370   S108; *Pfdhps* A437, K540, A581, A613; *Pfkelch13* C580), Dd2 (*Pfmdr1* YFD; *Pfcrt* K76T;

371   *Pfdhfr* N51I, C59R, S108N; *Pfdhps* A437G) HB3 (*Pfmdr1 NYD*; *Pfcrt* K76; *Pfdhfr* N51, C59,

372   S108N; *Pfdhps* A437G, K540, A581, A613) Tm90C6B (*Pfmdr1 NYD*; *Pfcrt* K76; *Pfdhfr* N51,

373   C59R *; Pfdhps* A437, K540, A581G*; Pfmdr 1 NYD*) and MRA1236 (*Pfkelch13* C580Y).

374 **DNA Sequencing**

375 The *Pfkelch13* propeller domain was amplified using a *P. falciparum* specific protocol

376 described previously[55]. PCR products were visualized on a 2% agarose gel after

377 electrophoresis. Sequencing of PCR products was performed using an ABI 3730 sequencer

378 by Sanger using a protocol established at CDC/Atlanta Malaria Genomic laboratory (Applied

379 Biosystems, Foster City, CA).

380 **Data Analysis**

381 The HRM result was analyzed using the LightCycler 96 application software version

382 1.1.0.1320. The *Pfkelch13* sequence data was analyzed using the Geneious software

383 (www.geneious.com). A cutoff of quality score HQ>30% was applied to all sequences.

384 Polymorphisms were considered if both the forward and reverse strands carried a mutation

385 and matched the quality score cut off.

386 **Haplotype Analyses**

387 A subset of 231 monogenomic (single-strain) samples collected from febrile, clinic-reporting

388 patients between 2006 and 2019 from Pikine, Thiès, and Kedougou were previously whole

389 genome sequenced using next-generation Illumina short reads. These sequences excluded

390 polygenomic (multiple strain) infections and avoided repeated sequencing of clones using a

391 24-SNP molecular barcode.

392 Briefly, short-reads were aligned to the *P. falciparum* 3D7 reference genome (PlasmoDB v.

393 28) using BWA-mem and Picard Tools. Variants were called using HaplotypeCaller in GATK

394 v3.5. Our whole genome sequence analyses focused on a set of 577,487 SNPs spread

395 throughout the core region of the genome. Bifurcation plots and extended haplotypes were

396 calculated using *rehh 2.0*[56].

397 These whole genome sequences were used to examine the genomic region surrounding

398 *Pfcrt, Pfdhfr,* and *Pfdhps*. Genomic regions were defined as the region 100kb upstream and

399   downstream of the starting and ending boundaries of each gene. The gene boundaries for

400   *Pfcrt, Pfdhfr,* and *Pfdhps* were obtained from Plasmodb (Plasmodb.org).

401   For each genomic region surrounding *Pfcrt, Pfdhfr,* and *Pfdhps*, samples and variant sites

402   were filtered by 1) excluding samples with > 50% unusable data in the examined genomic

403   region, 2) retaining sites with < 10% unusable data in the remaining samples, and 3) further

404   excluding samples with > 5% unusable data in the retained sites. Unusable data was defined

405   as any site with missing data (failed to be genotyped), or a site that was heterozygous or

406   triallelic. These filters were applied separately across all sample years, for samples collected

407   before 2014 (pre-SMC), and for samples collected after 2014 (post-SMC).

408   When applied across all sample years, the *Pfcrt* genomic region included 171 samples and

409   173 SNPs, the *Pfdhfr* genomic region included 170 samples and 85 SNPs, and the *Pfdhps*

410   genomic region included 182 samples and 83 SNPs. When applied on the pre-SMC data, the

411   *Pfcrt* genomic region included 64 samples and 21 SNPs, the *Pfdhfr* genomic region included

412   54 samples and 27 SNPs, and the *Pfdhps* genomic region included 51 samples and 75

413   SNPs. The majority of these samples were collected after 2010. For the post-SMC samples,

414   the *Pfcrt* genomic region included 114 samples and 213 SNPs, the *Pfdhfr* genomic region

415   included 170 samples and 95 SNPs, and the *Pfdhps* genomic region included 127 samples

416   and 89 SNPs (**Fig S5**).

417   **Generalized Additive Model**

418   Binomial generalized additive models (GAMs) were fit using the R package *mcgv* (v1.8-40).

419   The GAM quantifies the relationship between mutation frequency and sampling year across

420   all sites, while considering sample size and sampling origin. The structure of the GAM was

421   defined as:

$$g(proportion_{mutation}) = s(year, k) + \beta_1 samplesize + \beta_2 sampleorigin + \beta_3 origin + \beta_4 origin$$

422   where $proportion_{mutation}$ is the proportion of samples with the mutant allele, $s(year, k)$

423   is a smoothing spline function for the sample year. The *k* is the degrees of freedom used in

424   the smoothing spline function. The other covariates are binary categorical variables

425   specifying sample origin. Kolda and Kaolack were not included in the model because they

426   were sampled for less than three years.

427   **H12 and H2/H1 Analyses**

428   Genotypes were called for sequenced samples at 149,582 SNP sites, sites that were

429   chosen as reliable based on the full Pf3k dataset; details of the filtering are described in

430   another manuscript[57]. For this analysis, an additional 10,387 SNPs were eliminated because

431   of incompatible allele calls for 2019 and 2020 data (although only the former are being

432   reported here). These were then further filtered to remove sites that were monomorphic or

433   rare in our dataset, as well as filtered to remove densely packed sites. Specifically, a

434   threshold on the minimum minor allele frequency was set at 0.5%, while the minimum

435   spacing between markers was 20 bp and the maximum number of SNPs allowed in a 2 kb

436   window was 12. Within these restrictions, SNPs were prioritized by minor allele frequency.

437   The remaining 43,846 SNPs were used for analysis.

438   Rather than calculating these statistics directly from sequence data, however, we instead

439   based them on shared chromosome segments that were identified as being identical by

440   descent. Haplotype sharing among parasites was determined by first identifying chromosome

441   segments that were identical by descent (IBD) between each pair of parasites, using the

442   program hmmIBD (version 2.0.4)[58]. Because in hmmIBD, the threshold detecting IBD

443   segments between two parasites depends on their genome-wide relatedness, a modified

444   version of the program was used which fixed the genome-wide IBD fraction at 20%. In this

445   way, a determination of local IBD status could be made without bias by the parasites' overall

446   relatedness. We adopted this IBD approach because the hidden Markov model that it is

447   based on is well suited to identifying closely related haplotypes in our dataset. It takes into

448   account differing SNP frequencies, does not rely on arbitrary window sizes, and incorporates

449   into the model sequencing error and missing data.

450   At each SNP locus, haplotypes were defined by clustering samples that were related to one

451   another. Clustering was performed via a greedy algorithm as follows. For a pair of samples

452   IBD at a SNP site:

453   ▫   If neither is already in a cluster, form a new cluster.

454   ▫   If both are already in the same cluster, do nothing.

455   ▫   If they are already in different clusters, merge the clusters if 40% of pairwise

456   comparisons are IBD.

457   ▫   If one is in a cluster, add the other if it is IBD with at least 40% of existing samples in

458   the cluster. Otherwise, start a new cluster.

459   The resulting clusters are defined as the set of haplotypes at that locus. If we label the

460   population frequency of these haplotypes as p_1, p_2, p_3, etc., we then calculated H1, H2, and

461   H12[20,59]:

$$H_1 = p_1^2 + p_2^2 + \cdots$$
$$H_2 = p_2^2 + p_3^2 + \cdots$$
$$H_{12} = 2p_1 p_2 + p_1^2 + p_2^2 + p_3^2 + \cdots$$

462   H12 treats the two most common haplotypes as a single haplotype. In these calculations,

463   singleton haplotypes are omitted since their population frequency is likely to be much lower

464   than their sample frequency.
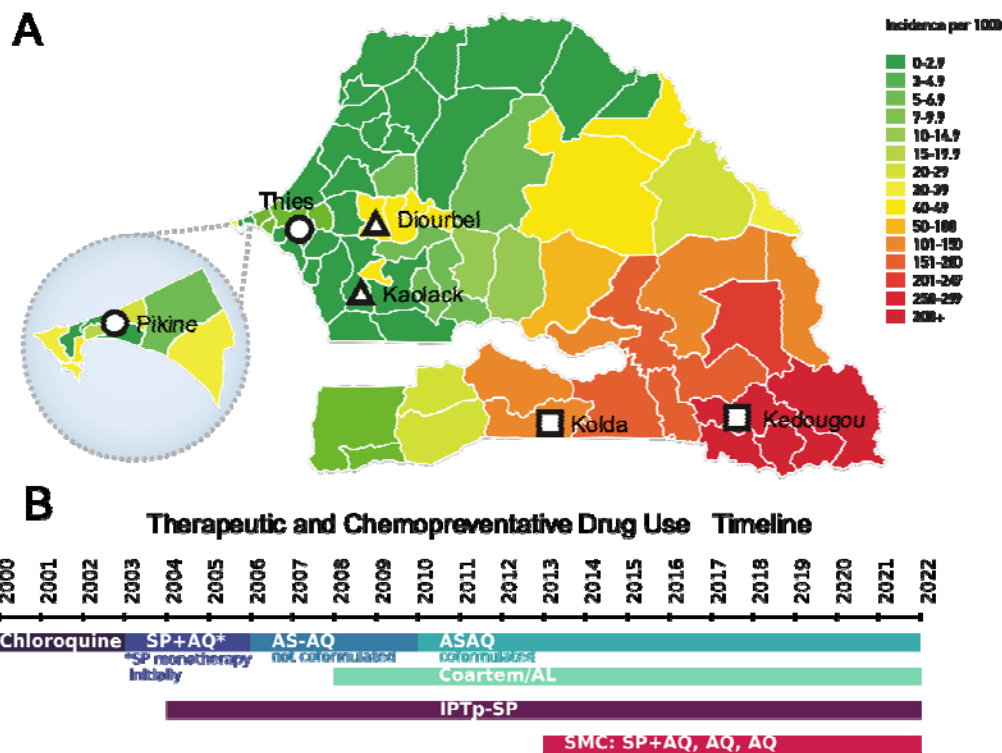
465

466   **Disclosure Statement**

467   The findings and conclusions in this paper are those of the authors

468   and do not necessarily represent the official position of the U.S. Centers for Disease Control

469   and Prevention.

470

471   **Ethics statement**

479   **Figures**

480

481   **Fig 1**: **Study design and Senegal drug history A**) Map of Senegal highlighting the different

482   study locations and their corresponding transmission levels in 2019. Each region is colored

483   by transmission intensity, with red indicating high transmission and green indicating low.

484   Squares denote sampled regions that started SMC in 2014, triangles those that started in

485   2019, and circles those that have not implemented SMC. **B**) Therapeutic and

486   chemopreventive drug use in Senegal. Therapeutic drug use in *blue/green*, chemopreventive

487   drug use in *red/purple*. SP = Sulfadoxine-Pyrimethamine, AQ = amodiaquine, ASAQ =

488   Artesenuate/Amodiaquine, Coartem/AL = Coformulated Artemether Lumefantrine, IPTp-SP =

489   Intermittent preventative therapy in pregnant women using SP, SMC = Seasonal malaria

490   chemoprevention.

491
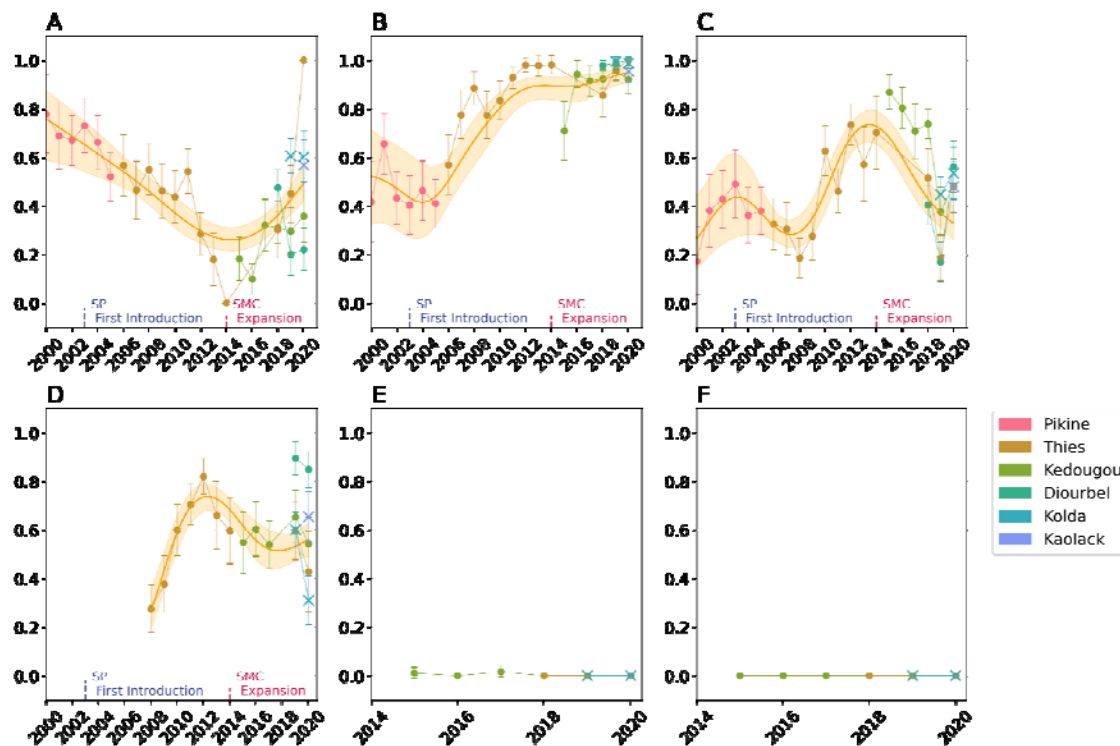
Fig 2. **SNP-based Molecular Surveillance Results.** Frequencies for **A**) *Pfcrt* K76T, **B**)

Pfdhfr triple mutant (N51C, C59R, S108N), **C**) *Pfdhps* A437G, **D**) *Pfmdr1* $N_{86}F_{184}D_{1246}$

haplotype (N86Y, Y184F, D1246Y), **E**) *Pfkelch13* A578S, and **F**) *Pfkelch13* C580Y. The

scatterplots show the observed frequencies and their 95% binomial confidence interval.

Model predictions from a calibrated generalized additive model and the 95% confidence

intervals are shown in orange. The model was calibrated with data from Pikine, Thiès,

Diourbel, and Kedougou (denoted with circles). The data from Kolda and Kaolack (denoted

with X) were not used for model calibration. Model predictions were not generated for the

*Pfkelch13* mutations due to their complete or near-complete absence in the data.

501

502

503

504

505
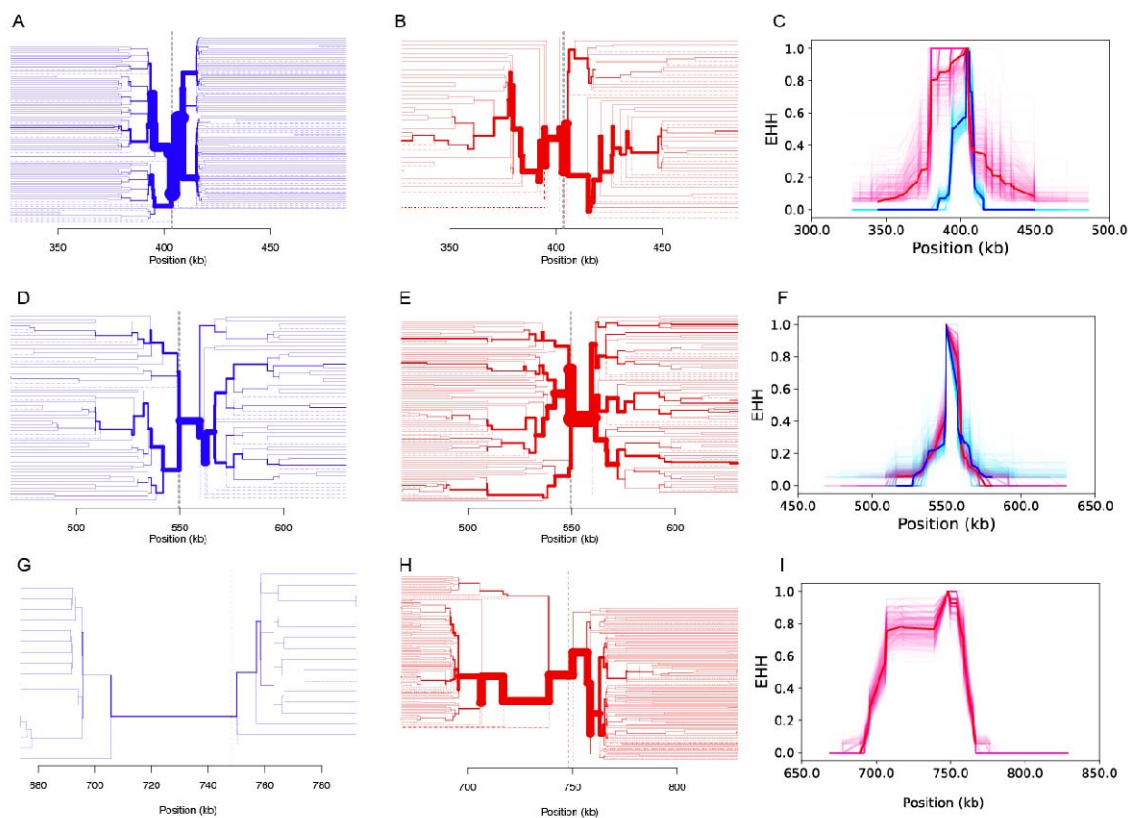
Fig 3 Evidence of selection at *Pfcrt, Pfdhps, and Pfdhfr*. Extended haplotype plots for the

A-C) *Pfcrt* K76T locus, **D-F**) *Pfdhps* A437G locus, and **G**) the *Pfdhfr* triple mutant. Red is

used for the resistance allele (*Pfcrt* K76T*, Pfdhps* A437G*,* and *Pfdhfr* triple mutant) while blue

is used for the sensitive allele (*Pfcrt* K76*, Pfdhps* A437*, Pfdhfr* triple sensitive). Column 1 (**A,**

D, G) used samples collected before and after the implementation of SMC. Column 2 (**B, E**)

used samples collected before SMC (before 2014), and Column 3 (**C**, **F**) used samples

collected after SMC (after 2014). The solid red and blue lines are the EHH estimates

obtained from using all available samples in the category. The lighter pink and blue traces

are bootstrapped EHH estimates obtained by randomly downsampling fifty samples. For **G-I**,

samples with mixed *Pfdhfr* genotypes were excluded.

516

517
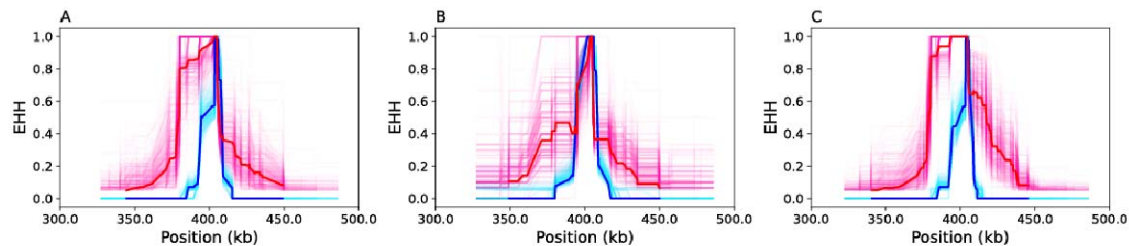
Fig 4 Temporal shifts in selection for *Pfcrt* K76T. Extended haplotype plots for the *Pfcrt*

K76T locus using **A)** all collected samples, **B**) samples collected before or during 2014, and

C) samples collected after 2014. The solid red and blue lines are the EHH estimates

obtained from using all available samples in the category. The lighter pink and blue traces

are bootstrapped EHH estimates obtained by randomly downsampling fifty samples. Note

that **Fig 4A** is the same as **Fig 3C**.

Table 1 Table of the molecular markers examined and their corresponding drug resistances

| Gene	SNPs assayed	Expected Drug Resistance
Pfcrt	K76T	Chloroquine, Amodiaquine
PfKelch13	A578S, C580Y	Artemisinin
Pfdhps	A437G, K540E, A581G, A613T/S	Sulfadoxine
Pfdhfr	N51C, C59R, S108N	Pyrimethamine
Pfmdr1	N86Y, Y184F, D1246Y	Multiple, including Amodiaquine, Mefloquine, Chloroquine, Artemether-Lumefantrine

525

526

527   **Supplemental Figures**
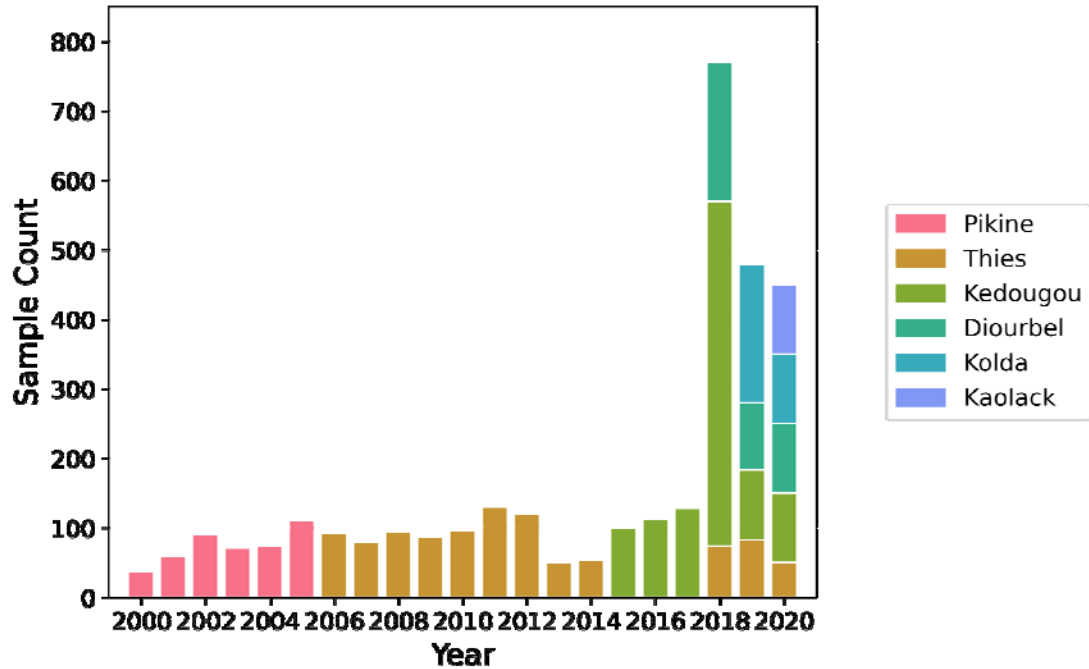
528

529 **Fig S1**. **Sample sizes for SNP-based molecular surveillance.** Sample size per year per

530 region for the SNP-based molecular surveillance.

531
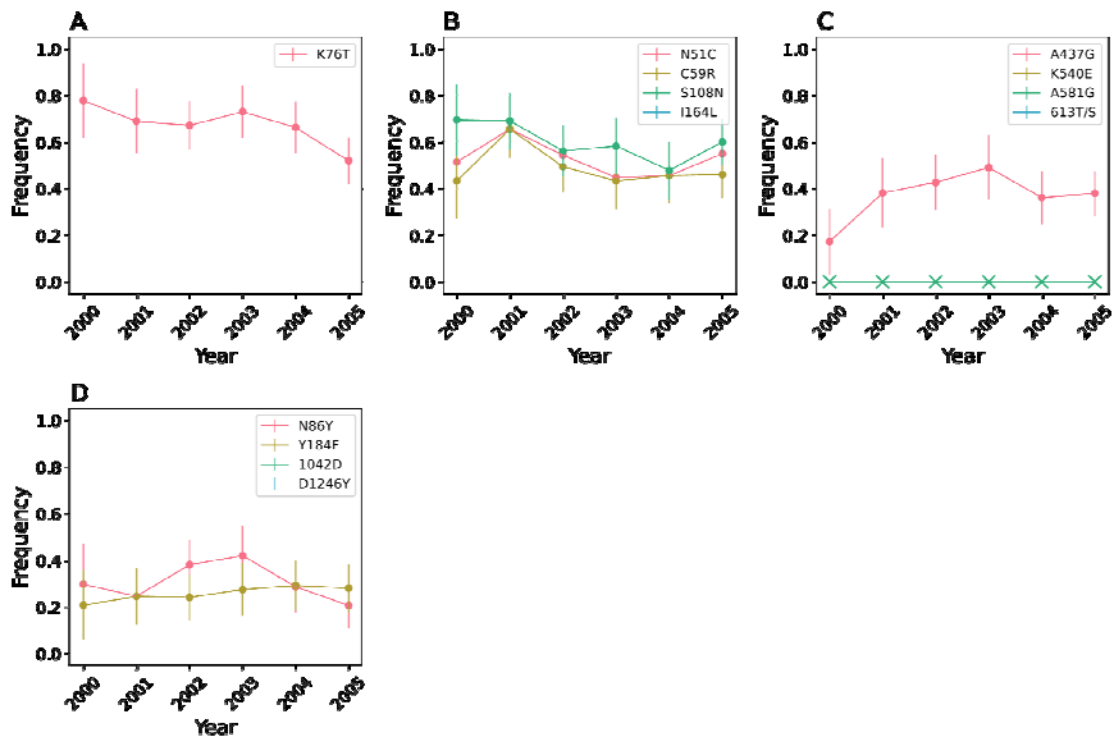
532

533   **Fig S2. SNP-based molecular surveillance in Pikine** for **A**) Pfcrt, **B**) *Pfdhfr*, **C**) *Pfdhps* and

534   **D**) Pfmdr1. The *Pfkelch13* SNPs were not examined in Pikine. Error bars indicate two

535   binomial standard deviations from the mean. X's denote years where samples were collected

536   but the mutation was not observed. Gaps in the data were because samples were not

537   collected for that year.
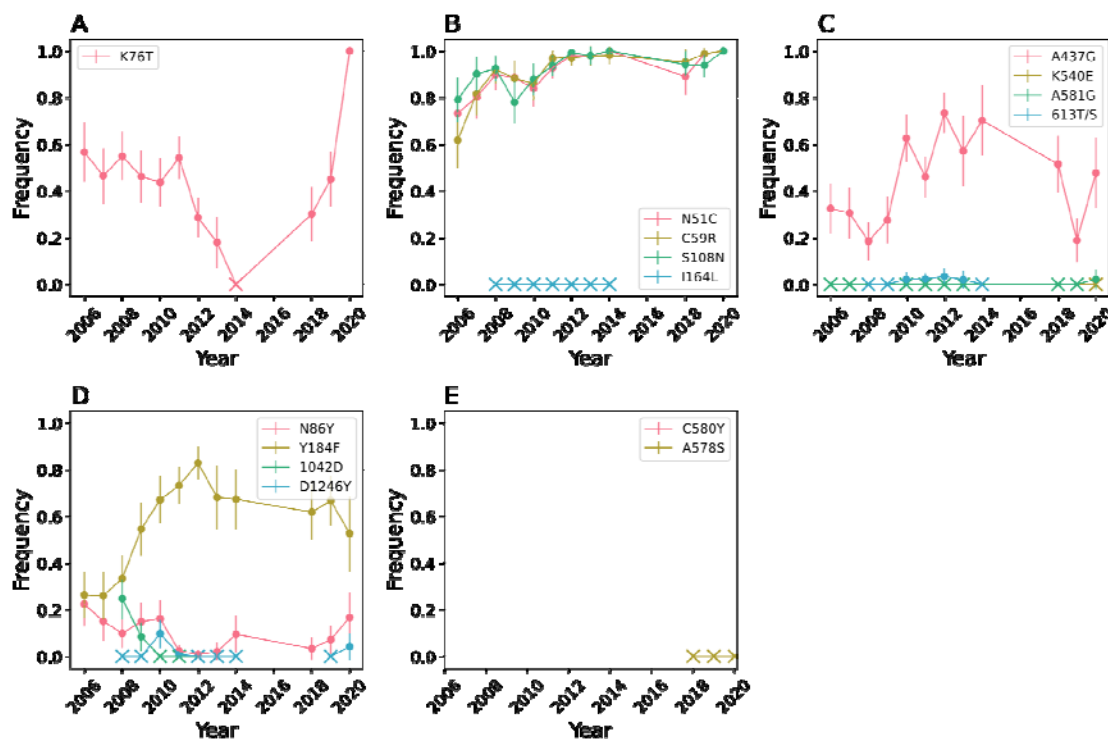
538

539   **Fig S3. SNP-based molecular surveillance in Thies** for **A**) Pfcrt, **B**) *Pfdhfr*, **C**) *Pfdhps* and

540   **D**) Pfmdr1, and **E**) *Pfkelch13*. Error bars indicate two binomial standard deviations from the

541   mean. X's denote years where samples were collected but the mutation was not observed.

542   Gaps in the data were because samples were not collected for that year.

543

544
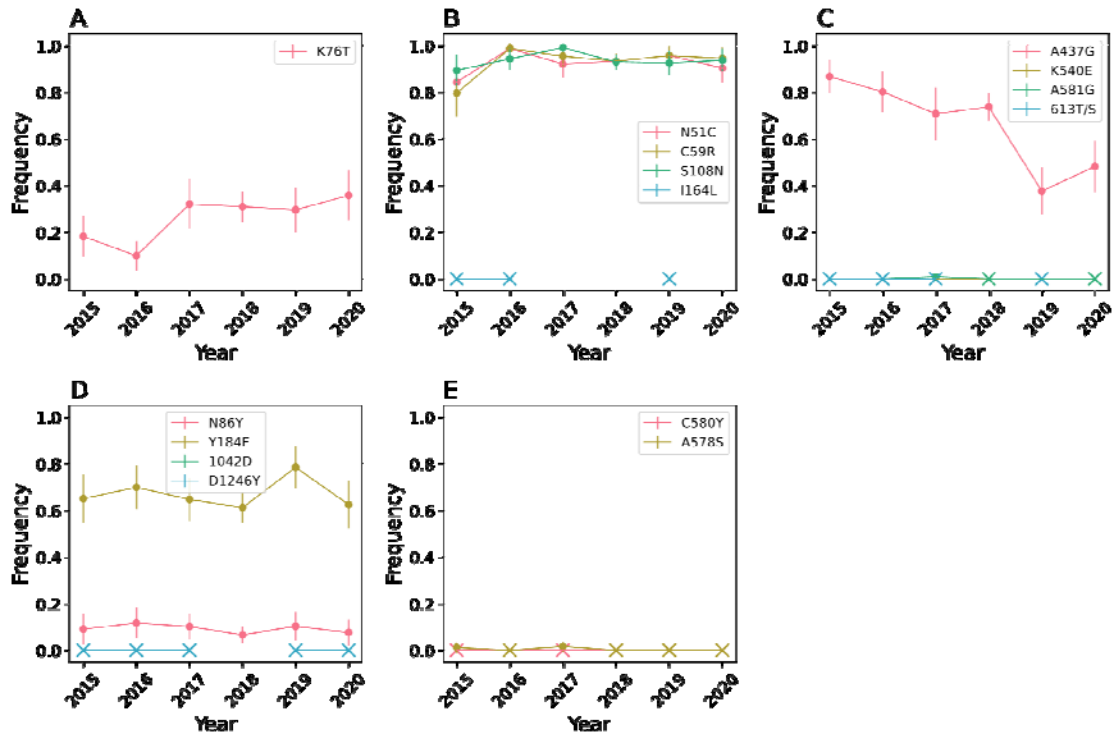
Fig S4. SNP-based molecular surveillance in Kedougou for **A**) Pfcrt, **B**) *Pfdhfr*, **C**)

Pfdhps, **D**) Pfmdr1, and **E**) *Pfkelch13*. Error bars indicate two binomial standard deviations

from the mean. X's denote years where samples were collected but the mutation was not

observed. Gaps in the data were because samples were either not collected or not

genotyped for that year.

550
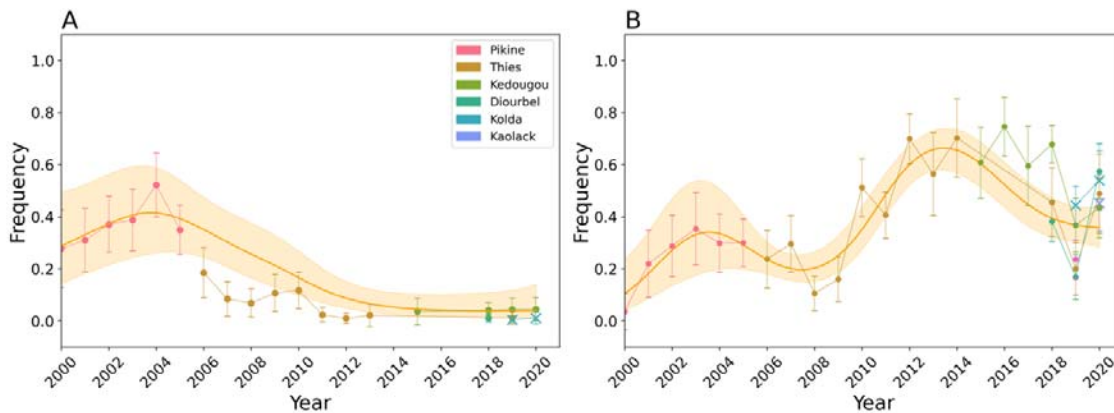
Fig S5. A) Frequency of *Pfdhfr* triple sensitive (N51, C59, S108) parasites. **B**) Frequency of

"quadruple" (*Pfdhfr* triple mutant + *Pfdhps* A437G) parasites. The scatterplots show the

observed frequencies and their 95% binomial confidence interval. Model predictions from a

calibrated generalized additive model and the 95% confidence intervals are shown in orange.

The model was calibrated with data from Pikine, Thiès, Diourbel, and Kedougou (denoted

556 with circles). The data from Kolda and Kaolack (denoted with X) were not used for model
557 calibration.
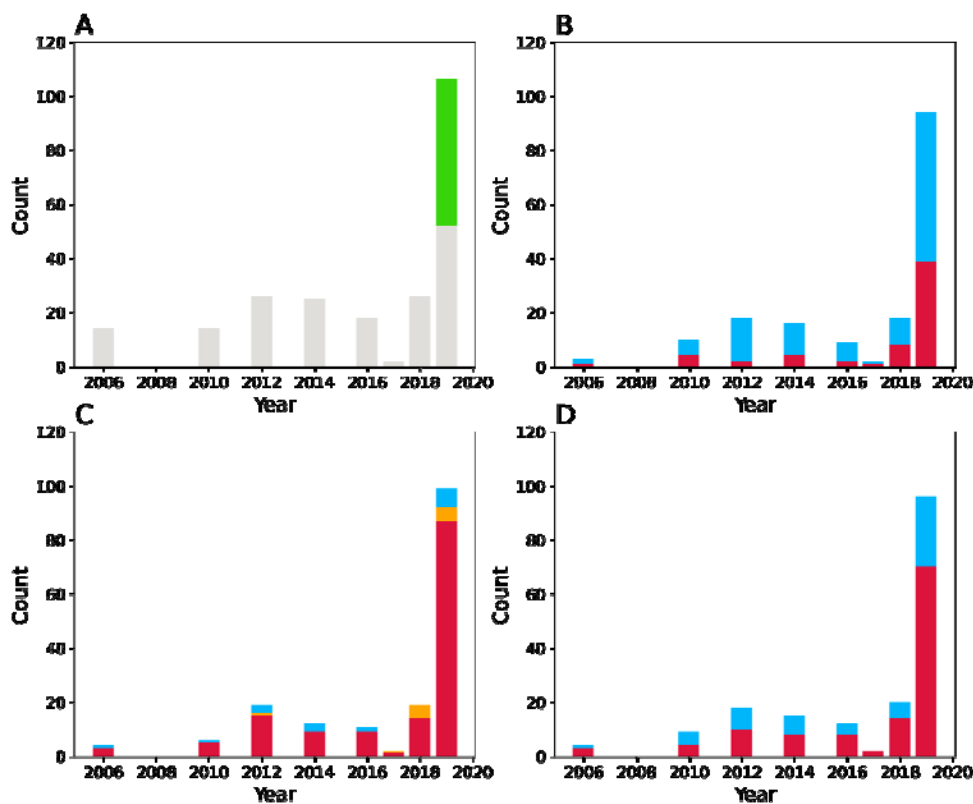
558
559 **Fig S6 Sampling distribution for our whole genome sequence collection** (**A**). Grey
560 indicates the sample came from Thiès. Green indicates the sample came from Kedougou.
561 Sampling distributions for **B**) the *Pfcrt* genomic region, **C**) the *Pfdhfr* genomic region, and **D**)
562 the *Pfdhps* genomic regions. For **B** and **D**, blue denotes samples with the sensitive allele and
563 red indicates those with the resistance allele. For **C**, red denotes samples that are *Pfdhfr*
564 triple mutant, blue indicates those that are *Pfdhfr* triple sensitive, and orange indicates those
565 with a mix of resistant and sensitive alleles at the three examined *Pfdhfr* loci.
566
567
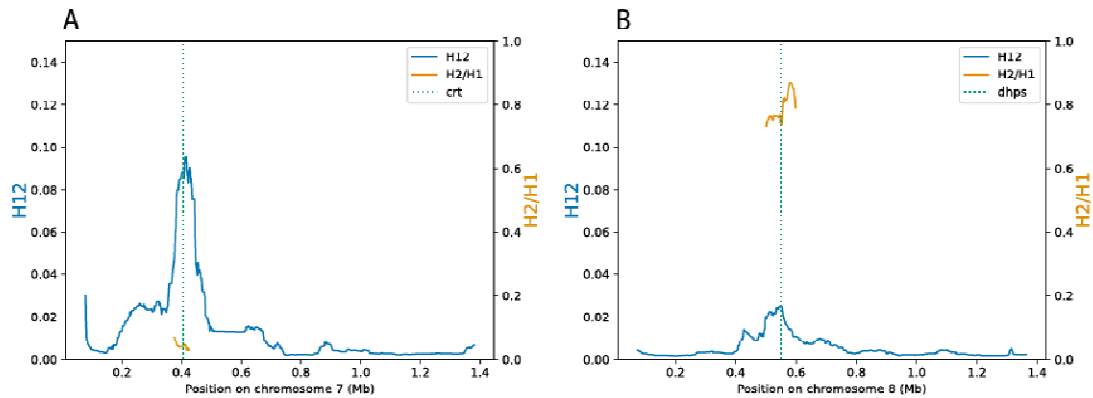
Fig S7 Evidence of Hard and Soft Sweeps H12 (*blue*, left y-axis) and H2/H1 (*orange*, right y-axis) statistics for **A**) chromosome 7 and **B**) chromosome 8. The dotted green lines show the location of *Pfcrt* or *Pfdhps*.
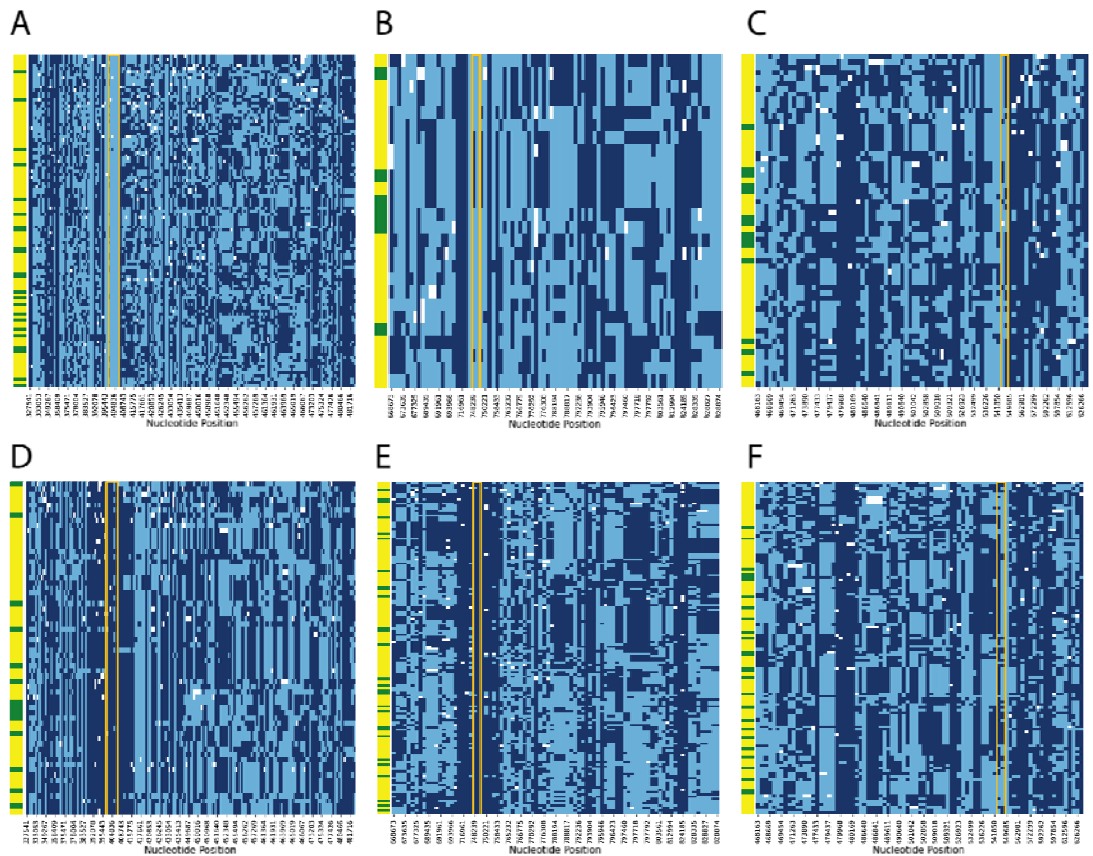
Fig S8. SNPs used to define genomic haplotypes. Genomic haplotypes surrounding the wild-type mutations: **A**) *Pfcrt* K76, **B**) *Pfdhfr* C59, **C**) *Pfdhps* A437 and the drug resistance mutations: **D**) *Pfcrt* K76T, **E**) *Pfdhfr* C59R, **F**) *Pfdhps* A437G. Each row represents a sample. The left most column indicates whether the sample was collected before 2014 (*green*) or

578   after 2014 (*yellow*). Alleles corresponding to the 3D7 reference are indicated by *light blue*

579   and alleles corresponding to the alternative allele are indicated by *dark blue*. White

580   corresponds to missing data. The orange boxes highlight the boundaries of the *Pfcrt* (**A/D**),

581   *Pfdhfr* (**B/E**), and *Pfdhps* (**C/F**) genes,

582
583
584
585   **Works Cited**

586   1.   World Health Organization. WHO Malaria World Report. (2021).

587   2.   World Health Organization. *World malaria report 2021*. (2021).

588   3.   World Health Organization. Report on antimalarial drug efficacy, resistance and response 10
589   years of surveillance (2010-2019). 64.

590   4.   Marwa, K. *et al.* Therapeutic efficacy of artemether-lumefantrine, artesunate-amodiaquine
591   and dihydroartemisinin-piperaquine in the treatment of uncomplicated Plasmodium
592   falciparum malaria in Sub-Saharan Africa: A systematic review and meta-analysis. *PLoS One*
593   **17**, e0264339 (2022).

594   5.   Sudathip, P. *et al.* Progress and challenges of integrated drug efficacy surveillance for
595   uncomplicated malaria in Thailand. *Malar J* **20**, 1–16 (2021).

596   6.   Plowe, C. v. Malaria chemoprevention and drug resistance: a review of the literature and
597   policy implications. *Malaria Journal 2022 21:1* **21**, 1–25 (2022).

598   7.   WHO. *Malaria chemoprevention efficacy study protocol*. (2022).

599   8.   Srimuang, K. *et al.* Analysis of anti-malarial resistance markers in pfmdr1 and pfcrt across
600   Southeast Asia in the Tracking Resistance to Artemisinin Collaboration. *Malar J* **15**, 1–12
601   (2016).

602   9.   Cheng, W., Song, X., Tan, H., Wu, K. & Li, J. Molecular surveillance of anti-malarial resistance
603   pfcrt, pfmdr1, and pfk13 polymorphisms in African Plasmodium falciparum imported parasites
604   to Wuhan, China. *Malar J* **20**, 1–8 (2021).

605   10.   Nwakanma, D. C. *et al.* Changes in Malaria Parasite Drug Resistance in an Endemic Population
606   Over a 25-Year Period With Resulting Genomic Evidence of Selection. (2013)
607   doi:10.1093/infdis/jit618.

608   11.   Imwong, M. *et al.* Molecular epidemiology of resistance to antimalarial drugs in the Greater
609   Mekong subregion: an observational study. *Lancet Infect Dis* **20**, 1470–1480 (2020).

610   12.   Conrad, M. D. & Rosenthal, P. J. Antimalarial drug resistance in Africa: the calm before the
611   storm? *Lancet Infect Dis* **19**, e338–e351 (2019).

612   13.   Ndiaye, Y. D. *et al.* Genetic surveillance for monitoring the impact of drug use on Plasmodium
613   falciparum populations. *Int J Parasitol Drugs Drug Resist* **17**, 12–22 (2021).

614   14.   Stephan, W. Selective Sweeps. *Genetics* **211**, 5 (2019).

615   15.   Programme National de lutte Contre le Paludisme. *Bulletin Epidemiologique Annuel 2021 Du*
616   *Paludisme au Senegal.* (2021).

617   16.   Lozovsky, E. R. *et al.* Stepwise acquisition of pyrimethamine resistance in the malaria parasite.
618   *Proc Natl Acad Sci U S A* **106**, 12025–12030 (2009).

619   17.   Gil, J. P. & Krishna, S. pfmdr1 (Plasmodium falciparum multidrug drug resistance gene 1): a
620   pivotal factor in malaria resistance to artemisinin combination therapies.
621   *http://dx.doi.org/10.1080/14787210.2017.1313703* **15**, 527–543 (2017).

622   18.   Shafik, S. H., Richards, S. N., Corry, B. & Martin, R. E. Mechanistic basis for multidrug
623   resistance and collateral drug sensitivity conferred to the malaria parasite by polymorphisms
624   in PfMDR1 and PfCRT. *PLoS Biol* **20**, e3001616 (2022).

625   19.   Hermisson, J. & Pennings, P. S. Soft sweeps: molecular population genetics of adaptation from
626   standing genetic variation. *Genetics* **169**, 2335–2352 (2005).

627   20.   Harris, A. M., Garud, N. R. & Degiorgio, M. Detection and Classification of Hard and Soft
628   Sweeps from Unphased Genotypes by Multilocus Genotype Identity. *Genetics* **210**, 1429
629   (2018).

630   21.   Wootton, J. C. *et al.* Genetic diversity and chloroquine selective sweeps in Plasmodium
631   falciparum. *Nature 2002 418:6895* **418**, 320–323 (2002).

632   22.   Ndiaye, D. *et al.* Polymorphism in dhfr/dhps genes, parasite density and ex vivo response to
633   pyrimethamine in Plasmodium falciparum malaria parasites in Thies, Senegal. *Int J Parasitol*
634   *Drugs Drug Resist* **3**, 135–142 (2013).

635   23.   Ndiaye, D. *et al.* Mutations in Plasmodium falciparum dihydrofolate reductase and
636   dihydropteroate synthase genes in Senegal. *Trop Med Int Health* **10**, 1176 (2005).

637   24.   Ecker, A., Lehane, A. M., Clain, J. & Fidock, D. A. PfCRT and its role in antimalarial drug
638   resistance. *Trends Parasitol* **28**, 504 (2012).

639   25.   Trape, J. F. *et al.* Impact of chloroquine resistance on malaria mortality. *Comptes Rendus de*
640   *l'Academie des Sciences - Serie III* **321**, 689–697 (1998).

641   26.   Fröberg, G. *et al.* Assessing the cost-benefit effect of a plasmodium falciparum drug resistance
642   mutation on parasite growth in vitro. *Antimicrob Agents Chemother* **57**, 887–892 (2013).

643   27.   Mulenga, M. C. *et al.* Decreased prevalence of the Plasmodium falciparum Pfcrt K76T and
644   Pfmdr1 and N86Y mutations post-chloroquine treatment withdrawal in Katete District,
645   Eastern Zambia. *Malar J* **20**, 1–8 (2021).

646   28.   Pelleau, S. *et al.* Adaptive evolution of malaria parasites in French Guiana: Reversal of
647   chloroquine resistance by acquisition of a mutation in pfcrt. *Proc Natl Acad Sci U S A* **112**,
648   11672–11677 (2015).

649   29.   Laufer, M. K. *et al.* Return of Chloroquine-Susceptible Falciparum Malaria in Malawi Was a
650   Reexpansion of Diverse Susceptible Parasites. *J Infect Dis* **202**, 801–808 (2010).

651   30.   Verity, R. *et al.* The impact of antimalarial resistance on the genetic structure of Plasmodium
652   falciparum in the DRC. *Nature Communications 2020 11:1* **11**, 1–10 (2020).

653   31.   Foguim, F. T. *et al.* Prevalence of mutations in the Plasmodium falciparum chloroquine
654   resistance transporter, PfCRT, and association with ex vivo susceptibility to common anti-
655   malarial drugs against African Plasmodium falciparum isolates. *Malar J* **19**, 1–9 (2020).

656   32.   Ochong, E. O., van den Broek, I. V. F., Keus, K. & Nzila, A. Short Report: Association Between
657   Chloroquine and Amodiaquine Resistance and Allelic Variation in the Plasmodium falciparum
658   Multiple Drug Resistance 1 Gene and the Chloroquine Resistance Transporter Gene in Isolates
659   From the Upper Nile in Southern Sudan. *Am J Trop Med Hyg* **69**, 184–187 (2003).

660   33.   Adamu, A. *et al.* Plasmodium falciparum multidrug resistance gene-1 polymorphisms in
661   Northern Nigeria: implications for the continued use of artemether-lumefantrine in the
662   region. *Malar J* **19**, 1–10 (2020).

663   34.   Diallo, M. A. *et al.* Efficacy and safety of artemisinin-based combination therapy and the
664   implications of Pfkelch13 and Pfcoronin molecular markers in treatment failure in Senegal. *Sci*
665   *Rep* **10**, (2020).

666   35.   Quan, H. *et al.* High multiple mutations of Plasmodium falciparum-resistant genotypes to
667   sulphadoxine-pyrimethamine in Lagos, Nigeria. *Infect Dis Poverty* **9**, (2020).

668   36.   *U.S. President's Malaria Initiative Senegal Malaria Operational Plan FY 2020*. (2020).

669   37.   Zupko Id, R. J. *et al.* Long-term effects of increased adoption of artemisinin combination
670   therapies in Burkina Faso. *PLOS Global Public Health* **2**, e0000111 (2022).

671   38.   Nguyen, T. D., Tran, T. N.-A., Parker, D. M., White, N. J. & Boni, M. F. Antimalarial mass drug
672   administration in large populations and the evolution of drug resistance. *bioRxiv*
673   2021.03.08.434496 (2021) doi:10.1101/2021.03.08.434496.

674   39.   Okell, L. C. *et al.* Emerging implications of policies on malaria treatment: genetic changes in
675   the Pfmdr-1 gene affecting susceptibility to artemether-lumefantrine and artesunate-
676   amodiaquine in Africa. *BMJ Glob Health* **3**, 999 (2018).

677   40.   Kayode, A. T. *et al.* Polymorphisms in Plasmodium falciparum chloroquine resistance
678   transporter (Pfcrt) and multidrug-resistant gene 1 (Pfmdr-1) in Nigerian children 10 years
679   post-adoption of artemisinin-based combination treatments. *Int J Parasitol* **51**, 301–310
680   (2021).

681   41.   Taieb, F. *et al.* Hydroxychloroquine and Azithromycin Treatment of Hospitalized Patients
682   Infected with SARS-CoV-2 in Senegal from March to October 2020. *J Clin Med* **10**, (2021).

683   42.   *Senegal Population and Housing Census 2013*. (2013).

684   43.   Ndiaye, T. *et al.* Molecular epidemiology of Plasmodium falciparum by multiplexed amplicon
685   deep sequencing in Senegal. *Malar J* **19**, 403 (2020).

686   44.   Wong, W. *et al.* RH: a genetic metric for measuring intrahost Plasmodium falciparum
687   relatedness and distinguishing cotransmission from superinfection. *PNAS Nexus* **1**, 1–11
688   (2022).

689   45.   Jacob, C. G. *et al.* Genetic surveillance in the greater mekong subregion and south asia to
690   support malaria control and elimination. *Elife* **10**, (2021).

691   46.   Ariey, F. *et al.* A molecular marker of artemisinin-resistant Plasmodium falciparum malaria.
692   *Nature* **505**, 50–55 (2014).

693   47.   Miotto, O. *et al.* Genetic architecture of artemisinin-resistant Plasmodium falciparum. *Nat*
694   *Genet* **47**, (2015).

695   48.   Rasmussen, C., Ariey, F., Fairhurst, R. M., Ringwald, P. & Ménard, D. Role of K13 Mutations in
696   Artemisinin-Based Combination Therapy. *Clinical Infectious Diseases* **63**, 1680–1681 (2016).

697   49.   Schmedes, S. E. *et al.* Plasmodium falciparum kelch 13 Mutations, 9 Countries in Africa, 2014–
698   2018. *Emerg Infect Dis* **27**, 1902 (2021).

699   50.   Asua, V. *et al.* Changing Prevalence of Potential Mediators of Aminoquinoline, Antifolate, and
700   Artemisinin Resistance Across Uganda. *J Infect Dis* **223**, 985 (2021).

701   51.   Balikagala, B. *et al.* Evidence of Artemisinin-Resistant Malaria in Africa. *New England Journal*
702   *of Medicine* **385**, 1163–1171 (2021).

703   52.   Gruenberg, M., Lerch, A., Beck, H. P. & Felger, I. Amplicon deep sequencing improves
704   Plasmodium falciparum genotyping in clinical trials of antimalarial drugs. *Scientific Reports*
705   *2019 9:1* **9**, 1–12 (2019).

706   53.   WHO. WHO Guidelines for malaria - 25 November 2022. (2022).

707   54.   Daniels, R. *et al.* Methods to Increase the Sensitivity of High Resolution Melting Single
708   Nucleotide Polymorphism Genotyping in Malaria. *J Vis Exp* **2015**, 52839 (2015).

709   55.   Talundzic, E. *et al.* Genetic Analysis and Species Specific Amplification of the Artemisinin
710   Resistance-Associated Kelch Propeller Domain in P. falciparum and P. vivax. *PLoS One* **10**,
711   e0136099 (2015).

712   56.   Gautier, M., Klassmann, A. & Vitalis, R. rehh 2.0: a reimplementation of the R package rehh to
713   detect positive selection from haplotype structure. *Mol Ecol Resour* **17**, 78–90 (2017).

714   57.   Schaffner, S. F. *et al.* Malaria surveillance reveals parasite relatedness, signatures of selection,
715   and correlates of transmission across Senegal. *medRxiv* 2023.04.11.23288401 (2023)
716   doi:10.1101/2023.04.11.23288401.

717   58.   Schaffner, S. F., Taylor, A. R., Wong, W., Wirth, D. F. & Neafsey, D. E. hmmIBD: software to
718   infer pairwise identity by descent between haploid genotypes. *Malar J* **17**, 196 (2018).

719   59.   Garud, N. R., Messer, P. W., Buzbas, E. O. & Petrov, D. A. Recent Selective Sweeps in North
720   American Drosophila melanogaster Show Signatures of Soft Sweeps. *PLoS Genet* **11**, e1005004
721   (2015).

722

723